PHYSICAL REVIEW B, VOLUME 64, 161309(R)

Ultrafast carrier dynamics in nanocrystalline silicon

K. E. Myers,[1] Q. Wang,[2] and S. L. Dexheimer[1]
[1]*Department of Physics, Washington State University, Pullman, Washington 99164-2814*
[2]*National Renewable Energy Laboratory, Golden, Colorado 80401*
(Received 14 June 2001; published 8 October 2001)

We present studies of the ultrafast dynamics of photoexcited carriers in thin-film nanocrystalline silicon materials in which the degree of crystallinity has been systematically varied by controlling the deposition conditions. Femtosecond pump-probe measurements reveal a multicomponent response that can be understood in terms of the separate phases of the heterogeneous material. We observe a 240-fs exponential relaxation process associated with intraband carrier relaxation in the silicon crystallites, a response characteristic of bimolecular recombination in the amorphous silicon matrix, and a long-lived component assigned to grain-boundary states.

DOI: 10.1103/PhysRevB.64.161309 PACS number(s): 78.47.+p, 78.67.Bf

Thin-film hydrogenated nanocrystalline silicon (nc-Si:H), which is comprised of nanoscale crystallites of silicon embedded in a hydrogenated amorphous silicon (a-Si:H) matrix, has attracted a great deal of recent attention due to its potential optoelectronic applications as well as the interesting physical properties that result from its heterogeneous nature. This material is particularly promising for photovoltaic applications, especially given its high efficiency and resistance to the photoinduced degradation characteristic of thin-film amorphous silicon. Important material parameters for nc-Si:H include the size of the crystallites and the crystalline fraction, or ratio of the volumes of the crystalline and amorphous components. A key issue in the physics of this heterogeneous material is the extent to which its optical and electronic properties can be understood simply as a combination of the properties of the separate phases, and in particular, the role of the grain-boundary regions. We note that similar materials have sometimes been referred to in the literature as microcrystalline silicon (μc-Si) or as polycrystalline silicon; here we use the designation nc-Si, since this more accurately reflects the size scale of the crystalline inclusions.

Previous studies of the dynamics of photoexcited carriers in these and related materials on subpicosecond and longer time scales[1–3] have reported time-resolved responses qualitatively similar to those observed in thin-film amorphous silicon, suggesting that the disordered nature of the heterogeneous material is the dominant effect seen by the photoexcitations, but not providing a definitive understanding of the photophysics. In this work, we have carried out high sensitivity and high time-resolution measurements on a series of materials of systematically controlled composition, allowing us to definitively interpret the carrier dynamics in terms of contributions associated with each of the component phases of the heterogeneous material. Of particular interest is the new observation of an ultrafast, 240-fs relaxation process in nc-Si:H, which we have identified as carrier relaxation within the silicon crystallites through the dependence of its amplitude on composition and by direct comparison with the femtosecond optical response of bulk crystalline silicon. Also observed are an excitation density-dependent component consistent with the bimolecular recombination processes observed in a-Si:H, and a slowly relaxing component that likely includes contributions from grain-boundary states.

The nanocrystalline silicon thin films studied in these experiments were grown by the hot-wire chemical vapor deposition (HWCVD) technique, and the composition of the materials was controlled by variation of the hydrogen dilution ratio $R = H_2/SiH_4$ during deposition. The films were deposited at a substrate temperature of 240 °C on Corning 7059 glass, and the hydrogen dilution ratio was varied while maintaining a total gas pressure of 30 mTorr. The samples have been extensively characterized by x-ray diffraction as well as by Raman, photoluminescence, and optical spectroscopy. X-ray diffraction measurements indicate the presence of a crystalline component for $R > 3$, and x-ray measurements, together with Raman measurements, show that both the grain size and the crystalline fraction increase with R (Ref. 4). All of the nc-Si:H samples show nearly identical optical-absorption spectra,[5] with a monotonic increase over the measured range of 0.8–2.0 eV.

The properties of the samples are summarized in Table I. Average crystallite grain sizes are determined by x-ray diffraction along the (111) and (220) directions. These measurements indicate that the preferred growth direction changes with increasing dilution ratio, resulting in a variation of the crystallite shape with R. The composition of each sample is estimated from the relative intensities of Raman features associated with each component, as discussed in Ref. 4, and is expressed in terms of the percentage volume fractions X_c, X_a, and X_{gb} for the crystalline, amorphous, and grain-boundary phases, respectively. The Raman results demonstrate the variation of the material composition with R, though the values for the fractional compositions should be considered approximate: in contrast to the time-resolved op-

TABLE I. Properties of nc-Si:H as a function of dilution ratio R.

	Grain size (nm)		Vol. fraction, %		
R	(111)	(220)	X_c	X_{gb}	X_a
4	7.1	26.9	43	38	19
5	10.7	35.1	56	27	17
10	18.7	32.1	63	26	11

tical measurements, which sample the entire 1.4–2.4 μm thickness of the films, the Raman measurements were carried out at an excitation wavelength of 514.5 nm, giving a penetration depth of only ~200 nm in the nc-Si:H films. Detailed studies of nc-Si:H films[5] have shown that the structure varies with film thickness, with the region adjacent to the glass substrate forming a thin amorphous layer.

Time-resolved measurements of the carrier dynamics were carried out using a femtosecond pump-probe technique, in which a short pump pulse excites carriers in the sample and a time-delayed probe pulse measures the resulting change in transmission as a function of the pump-probe delay time. The optical pulses were generated using an amplified Ti:sapphire laser system operating at a repetition rate of 1 kHz. Pulses 35 fs in duration centered at 800 nm (1.55 eV) were used to excite the samples. Probe pulses of variable wavelength were produced by using a portion of the amplified 800-nm beam to generate a femtosecond white light continuum in a 1-mm thick sapphire plate, and the near-infrared components of the continuum were compressed using a fused-silica prism delay line to give an overall time resolution of ~40 fs in the pump-probe measurements. Wavelength resolution was achieved by spectrally filtering the probe beam with a 10-nm bandwidth interference filter after it had been transmitted through the sample. The pump beam was modulated with a mechanical chopper operating at a frequency of ~100 Hz, and the resulting change in the energy of the spectrally filtered probe beam was detected using lock-in amplification. For purposes of noise reduction, a separate reference beam was split off from the probe beam prior to its interaction with the sample. The reference beam was spectrally filtered in a manner identical to that used for the transmitted probe beam prior to detection by a separate, matched photodiode, also using ~100 Hz modulation and lock-in amplification. To correct the pump-probe signal for intensity fluctuations in the continuum at the selected probe wavelength, the signal was normalized by the reference amplitude at each delay time point, providing a significant improvement in the sensitivity of the measurements. For this study, all measurements were carried out at room temperature and with mutually perpendicular pump and probe polarizations. Pump-probe signals were measured over a range of pump intensities to ensure linearity of the response with respect to the initial excitation density.

Since the dynamics of the photoexcited carriers depend on excitation density, care was taken in the experimental design to minimize distortion of the measured pump-probe response by spatial inhomogeneity of the excited carrier distribution. The pump and probe beams were focused on the sample using a 9-cm focal length achromat, and the diameters of the beams were adjusted so that the probe beam sampled only the central portion of the pumped area, with Gaussian beam diameters at the sample of ~120 μm for the 800 nm pump beam and ~30 μm for the 940 nm component of the probe beam used in the measurements. To ensure the reproducibility of the alignment, the spatial overlap of the beams was set using a precision pinhole. Spatial variation of the density of photoexcited carriers across the depth of the sample was minimized by using optically thin films with optical densities of less than 0.1. Care was also taken to minimize distortion of the measured pump-probe response by thin-film interference effects. In general, excitation of carriers in a semiconductor will perturb both the real and imaginary parts of the index of refraction, and the measured change in transmission or reflection of a thin-film sample will include both of these effects due to the resulting modulation of the etalon response. In this study, we are interested in photoinduced changes in the absorption of the material, and accordingly, we have carried out the pump-probe measurements at conditions that correspond to a transmission maximum of the etalon response, largely eliminating contributions from modulation of the real part of the refractive index.[6] Since the samples have a small, but nonzero, variation in thickness over the area of the film, this condition could be met by choosing an appropriate position on each sample.

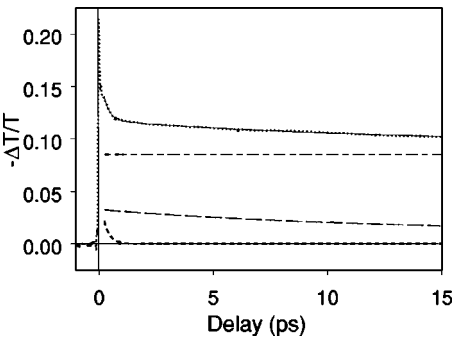

FIG. 1. Time-resolved negative differential transmittance of a nc-Si:H thin film with dilution ratio $R=4$ measured over a range of pump-probe delay times extending to 15 ps. The solid line represents a fit to the three-component model described in the text, and the dashed lines show the contributions of the individual components. [- - - exponential process, – – – bimolecular recombination, – - – - long-lived (constant) component].

Measurements of the time-resolved differential transmittance were carried out on nc-Si:H films prepared at hydrogen dilutions $R=4$, 5, and 10. For each sample, measurements were carried out over a range of pump fluences, corresponding to a range of initial excitation densities. In all of the materials, photoexcitation of carriers resulted in a net induced absorbance signal, which is presented in the figures as a negative differential transmittance, $-\Delta T/T$, where ΔT is the change in transmittance due to the action of the pump pulse, and T is the transmittance of the sample in the absence of the pump pulse. The response was probed at a detection wavelength of 940 nm (1.32 eV). In the small signal limit, the differential transmittance measurements are expected to be proportional to the photoinduced carrier population, and the time course of the signal reflects the dynamics of the photoexcited carrier distribution. The sharp features near $t=0$ include contributions from nonlinear effects that occur during the temporal overlap of the pump and probe pulses, and are excluded from the analysis of the population dynamics.

Representative data for the $R=4$ material over the first 15 ps of the delay range are presented in Fig. 1. The time-resolved response can be seen to include a rapid, subpicosecond component, together with a more slowly varying

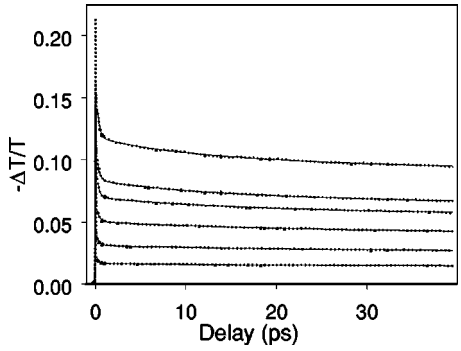

FIG. 2. Time-resolved negative differential transmittance of a nc-Si:H thin film with dilution ratio $R=4$, at initial carrier densities of approximately 2.4×10^{19} cm^{-3}, 1.8×10^{19} cm^{-3}, 1.5×10^{19} cm^{-3}, 1.2×10^{19} cm^{-3}, 9.0×10^{18} cm^{-3}, and 6.0×10^{18} cm^{-3}. The solid lines correspond to fits to the three-component model described in the text.

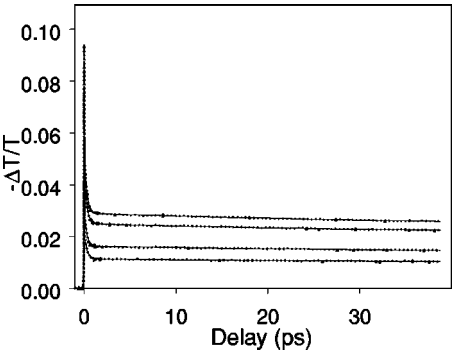

FIG. 3. Time-resolved negative differential transmittance of a nc-Si:H thin film with dilution ratio $R=10$, at initial carrier densities of approximately 1.8×10^{19} cm^{-3}, 1.5×10^{19} cm^{-3}, 1.2×10^{19} cm^{-3}, and 9.0×10^{18} cm^{-3}. The solid lines correspond to fits to the three-component model described in the text.

response. These dynamics are well characterized by a model consisting of three components,

$$n(t)=ae^{-t/\tau}+n_0/(1+n_0kt)+c, \tag{1}$$

which represent a population that undergoes fast exponential dynamics with a time constant τ, a population that undergoes bimolecular recombination with an associated rate constant k [the second term of the right-hand side of Eq. (1) corresponds to the solution to the rate equation $dn/dt=-kn^2$ with $n(t=0)=n_0$], and a component of amplitude c that decays slowly compared to the time scale of the measurements. The results of a fit to this model, together with traces corresponding to the three individual components, are shown along with the data in Fig. 1. As is discussed in more detail below, the fast 240-fs exponential component is identified as carrier relaxation within the silicon crystallites, and the component consistent with bimolecular recombination dynamics originates in the amorphous fraction of nc-Si:H. The component of amplitude c represents a response that decays slowly on the time scale of the measurements, and effectively appears constant within the 40 ps time scale investigated here. As discussed below, this component is identified with contributions from long-lived states, and may also include some contribution from lattice heating. Since we observe no pump-probe response at negative time delay, where the probe pulse precedes the pump pulse, we can conclude that the long-lived component completely recovers within the 1 kHz repetition rate of our laser system.

The time-resolved response measured over a 40 ps range at a series of initial excitation densities for $R=4$ nc-Si:H is shown in Fig. 2, together with the results of fits to Eq. (1). The dependence of the response on initial excitation density is accurately reflected by the model: the amplitudes a, c, and n_0 associated with each of the components increase in direct proportion to the initial density of photoexcited carriers, while the values of the parameters τ and k remain the same for all of the data traces. The dependence of the time-resolved differential transmittance on initial excitation density confirms that the component of the response that has an effective rate increasing with excitation density is consistent with a bimolecular recombination mechanism. For comparison, pump-probe measurements over a similar range of initial excitation densities on nc-Si:H samples with $R=10$ are presented in Fig. 3. Measurements on all of the samples give excellent fits to Eq. (1). All of the nc-Si:H materials yield consistent values for the exponential time constant $\tau=240$ (±10) fs and the bimolecular recombination constant $k\sim3\times10^{-9}$ cm^3/s, indicating that the associated components have the same physical origin in all samples. The relative amplitudes of the components vary systematically with sample composition, as can be seen in Table II, which presents the values of the amplitudes a, c, and n_0 as a fraction of the total signal amplitude for each sample composition.

The excellent fit between the data and the physical model represented by Eq. (1) allows the photoexcited carrier dynamics in nc-Si:H to be understood in terms of the component phases of the heterogeneous material, with separate carrier populations evident in the crystalline and amorphous phases. The fast, 240-fs exponential response is a new observation in nc-Si:H, and can be identified as originating within the silicon nanocrystallites. Comparing the different sample compositions, we find that the amplitude of the exponential component as a fraction of the total signal level increases with dilution ratio R, which correlates with increasing crystalline fraction and crystallite size. We have identified the fast exponential component as intraband carrier relaxation in the crystalline phase of the material by comparison with the time-resolved differential transmittance response measured directly in thinned crystalline silicon.[7] Excitation of carriers at 1.55 eV, well above the indirect gap of crystalline silicon of 1.1 eV, creates a nonequilibrium carrier distribution that is

TABLE II. Component amplitudes determined by fitting the time-resolved response to the three-component model of Eq. (1).

R	$a/(a+n_0+c)$	$n_0/(a+n_0+c)$	$c/(a+n_0+c)$
4	0.23±0.032	0.21±0.062	0.56±0.068
5	0.41±0.031	0.08±0.028	0.51±0.043
10	0.62±0.012	0.06±0.015	0.32±0.014

expected to relax to the band edge via phonon emission. Time-resolved differential transmittance measurements on thinned crystalline silicon probed at a detection wavelength of 940 nm (1.32 eV) show a bleach (increase in transmission) that forms with an exponential rise time of 240 fs and then remains constant on picosecond and longer time scales, consistent with the initially excited carriers relaxing to the indirect band edge. In nc-Si:H, the net differential transmittance signal is negative, so this rising bleach component appears as a fast exponential decay on top of the overall induced absorbance response. In the nc-Si:H materials studied here, the size of the crystallites is larger than the threshold of ~ 5 nm below which quantum confinement effects have been detected in silicon,[8] consistent with the observation of bulklike properties associated with the crystalline fraction of the material. We note that our measured time constant for the onset of the bleach in the differential transmittance measurements is consistent with transient components previously reported in the time-resolved reflectivity response of bulk crystalline silicon materials as seen in c-Si wafers[9] and silicon-on-sapphire thin films.[10]

The second term in Eq. (1) represents the time dependence of a carrier population n_0 that undergoes bimolecular recombination, giving rise to an effective decay rate that depends on excitation density. The resulting value of the bimolecular recombination constant k is consistent with that determined using a straightforward rate equation analysis of the pump-probe response in previous studies of a-Si:H and related materials.[11–14] Although the detailed nature of the relaxation processes in a-Si:H and related materials is still under discussion, the correspondence with the response characteristic of a-Si:H indicates that the excitation-density-dependent portion of the nc-Si:H response originates from the amorphous fraction of the material, and the relative amplitude of this response varies appropriately with dilution ratio R.

The constant c in Eq. (1) corresponds to a component that decays slowly on a picosecond time scale, effectively giving rise to a constant response on the measured time scale. This component is expected to include an offset of magnitude a from the residual bleach in the crystalline fraction, but clearly includes other contributions, since it is observed as a net induced absorbance. The component may include effects from lattice heating due to the photoexcited carriers, as observed in previous studies[11] on a-Si:H. However, the large amplitude of the slowly decaying response in nc-Si:H, together with the observed dependence of its relative amplitude on sample composition indicates that it includes additional contributions, likely from long-lived carrier states associated with the grain-boundary regions.

In conclusion, we have carried out systematic studies of the ultrafast dynamics of photoexcited carriers in nc-Si:H as a function of material composition. We find that the response can be understood in terms of contributions from the separate phases of the heterogeneous material, and we have identified a fast, 240-fs relaxation component associated with intraband carrier relaxation within the crystalline regions.

This work was supported by a subcontract from the U.S. Department of Energy National Renewable Energy Laboratory and by the National Science Foundation Division of Materials Research under Grant No. 9973615.

[1] M. Kubinyi, A. Grofcsik, and W.J. Jones, J. Mol. Struct. **408/409**, 121 (1997).

[2] G. Juska, M. Viliunas, K. Arlauskas, J. Stuchlik, and J. Kocka, Phys. Status Solidi A **171**, 539 (1999).

[3] J. Kudrna, P. Maly, F. Trojanek, J. Stepanek, T. Lechner, I. Pelant, J. Meier, and U. Kroll, Mater. Sci. Eng., B **69-70**, 238 (2000).

[4] G. Yue, J.D. Lorentzen, J. Lin, D. Han, and Q. Wang, Appl. Phys. Lett. **75**, 492 (1999).

[5] D. Han, G. Yue, J.D. Lorentzen, J. Lin, H. Habuchi, and Q. Wang, J. Appl. Phys. **87**, 1882 (2000).

[6] H.T. Grahn, C. Thomsen, and J. Tauc, Opt. Commun. **58**, 226 (1986).

[7] K. E. Myers and S. L. Dexheimer (unpublished).

[8] J. von Behren, T. von Buuren, M. Zacharias, E.H. Chimowitz, and P.M. Fauchet, Solid State Commun. **105**, 317 (1998).

[9] T. Sjodin, H. Petek, and H-L. Dai, Phys. Rev. Lett. **81**, 5664 (1998).

[10] F.E. Doany and D. Grischkowsky, Appl. Phys. Lett. **52**, 36 (1988).

[11] P.M. Fauchet, D. Hulin, R. Vanderhaghen, A. Mourchid, and J.W.L. Nighan, J. Non-Cryst. Solids **141**, 76 (1992).

[12] A. Esser, K. Seibert, H. Kurz, G.N. Parsons, C. Wang, B.N. Davidson, G. Lucovsky, and R.J. Nemanich, Phys. Rev. B **41**, 2879 (1990).

[13] I.A. Shkrob and R.A. Crowell, Phys. Rev. B **57**, 12 207 (1998).

[14] J.E. Young, B.P. Nelson, and S.L. Dexheimer, in *Amorphous and Heterogeneous Silicon Thin Films-2000*, edited by R. W. Collins *et al.*, Mater. Res. Soc. Symp. Proc. No. **609** (Materials Research Society, Pittsburgh, 2000), A20.1.